Mutation Research 751–752 (2013) 42–48

Contents lists available at ScienceDirect

Mutation Research/Fundamental and Molecular Mechanisms of Mutagenesis

journal homepage: www.elsevier.com/locate/molmut
Community address: www.elsevier.com/locate/mutres

Transplacental clastogenic and epigenetic effects of gold nanoparticles in mice

Roumen Balansky[a], Mariagrazia Longobardi[b], Gancho Ganchev[a], Marietta Iltcheva[a], Nikolay Nedyalkov[c], Petar Atanasov[c], Reneta Toshkova[d], Silvio De Flora[b], Alberto Izzotti[b,*]

[a] National Center of Oncology, Sofia, Bulgaria
[b] Department of Health Sciences, University of Genoa, Genoa, Italy
[c] Institute of Electronics, Bulgarian Academy of Sciences, Sofia, Bulgaria
[d] Institute of Experimental Morphology, Pathology and Anthropology with Museum, Bulgarian Academy of Sciences, Sofia, Bulgaria

ARTICLE INFO

Article history:
Received 22 March 2013
Received in revised form 1 August 2013
Accepted 23 August 2013
Available online 1 September 2013

Keywords:
Gold nanoparticles
Transplacental
Mouse fetus
Clastogenicity
microRNA expression

ABSTRACT

The broad application of nanotechnology in medicine, biology, and pharmacology is leading to a dramatic increase of the risk of direct contact of nanoproducts, among which gold nanoparticles (AuNP), with the human organism. The present study aimed at evaluating *in vivo* the genotoxicity of AuNPs with average size of 40 nm and 100 nm. A single intraperitoneal treatment of adult male and female Swiss mice (strain H) with AuNPs, at a dose of 3.3 mg/kg body weight, had no effect on the frequency of micronucleated polychromatic erythrocytes (MN PCEs) in bone marrow. Conversely, the transplacental treatment with AuNP-100 nm, but not with AuNP-40 nm, applied intraperitoneally at a dose of 3.3 mg/kg to pregnant mice on days 10, 12, 14, and 17 of gestation, resulted in a significant increase in the frequency of MN PCEs in both liver and peripheral blood of mouse fetuses. In parallel, the same treatment with AuNP-100 nm, but not with AuNP-40 nm, produced significant changes in microRNA expression. In particular, out of 1281 mouse microRNAs analyzed, 28 were dys-regulated more than two-fold and to a statistically significant extent in fetus lung, and 5 were up-regulated in fetal liver. Let-7a and miR-183 were significantly up-regulated in both organs. The data presented herein demonstrate for the first time the transplacental size-dependent clastogenic and epigenetic effects of AuNPs in mouse fetus, thus highlighting new aspects concerning the putative genotoxicity of AuNPs during a vulnerable period of life.

1. Introduction

The field of nanotechnology has become one of the most intensively growing areas of research. A wide spectrum of nanomaterials have been manufactured and used not only in industry but also in medicine, biology, pharmacology, and daily human life. A number of nanoparticles (NPs) are already in use or under investigation for their possible applications as drug and gene carriers and for the production of biocompatible materials as well as for medical monitoring, *in vitro* and *in vivo* diagnostics, and therapy of neoplastic diseases [1–4]. The increasing manufacturing and wide distribution of nanomaterials in human life may involve opportunities for direct contact with the human organism. Therefore, the resulting potential risk should be carefully evaluated in order to prove the safety of NPs.

The possible health hazard of NPs is mainly linked to their size, chemical composition and structure, shape, and surface charge. In particular, the particle size is a key feature defining their biological activity [5]. In most cases, smaller nanoparticles produce greater biological responses compared to their larger counterparts, due to differences in the surface/volume ratio. Despite the fact that nanotoxicology and nanogenotoxicology are newly emerging scientific disciplines, the data accumulated during the last years have clearly indicated that nanomaterials may possess toxic and genotoxic properties. For example, Landsiedel et al. [6] reported that, in 14 of 19 studies using the comet assay and in 12 of 14 studies using the micronucleus test, positive results were obtained by testing a variety of NPs, such as engineered TiO_2, cobalt chrome, ZnO, SiO_2, Fe(II) and (III), carbon nanotubes, and carbon black.

Special attention should be paid to gold nanoparticles (AuNPs), due to their potential medical applications, such as plasmon-based labeling and imaging, optical and electrochemical sensing, diagnostics and therapy for a number of diseases, including

Abbreviations: AuNPs, gold nanoparticles; miRNAs, microRNAs; MN, micronucleated; NP, nanoparticles; PCEs, polychromatic erythrocytes; NCEs, normochromatic erythrocytes.

* Corresponding author. Tel.: +39 010 3538522; fax: +39 010 3538504.
E-mail address: izzotti@unige.it (A. Izzotti).

0027-5107/$ – see front matter © 2013 Elsevier B.V. All rights reserved.
http://dx.doi.org/10.1016/j.mrfmmm.2013.08.006

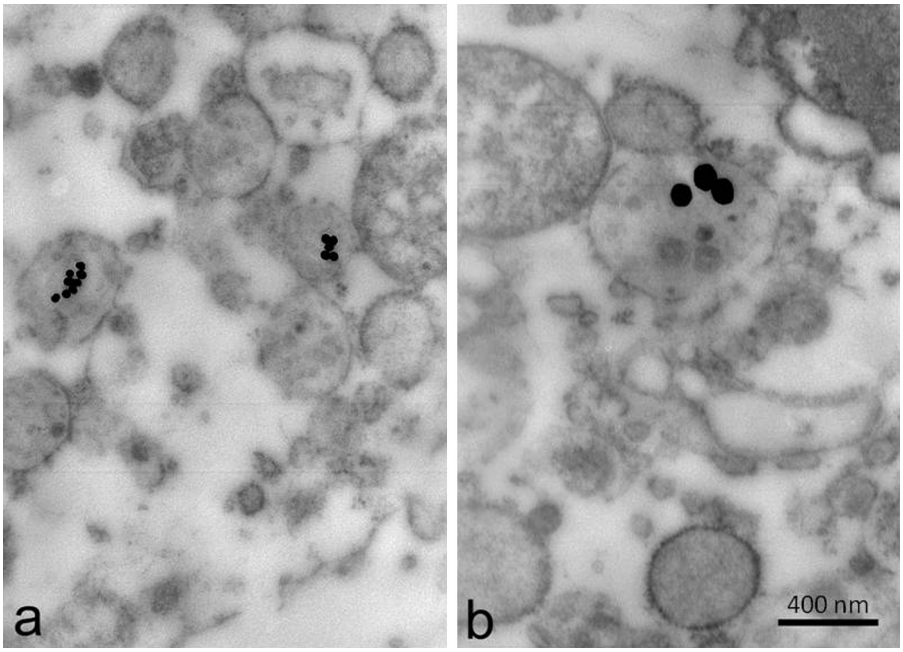

Fig. 1. Transmission electron microscope images of AuNPs of 40 nm (a) and 100 nm (b) in HeLa cells after 24 h of incubation.

cancer, Alzheimer's disease, hepatitis, arthritis, diabetes and others [2,7–11]. AuNPs have generally been regarded as bioinert, probably taking into account the stability of the bulk gold and its safety and biocompatibility [12]. However, some recent studies have reported that AuNPs might bind to DNA and produce cytotoxic effects [12–16]. Most of these studies were performed *in vitro*, which renders extrapolation to the human situation more difficult [12].

In the present study, we evaluated the genotoxic properties of AuNPs *in vivo* both by studying their capabilities to induce chromosome damage, as assessed by the MN test, and by evaluating their ability to epigenomically affect the post-transcriptional regulation of gene expression, as assessed by analyzing changes in miRNA expression spectra. Since exposure to nanoparticles during pregnancy might represent a health hazard not only to the mother but also to the fetus, we used a model involving the transplacental exposure of mice with AuNPs. It had previously been demonstrated that AuNPs, administered intravenously to rats, can cross the placenta and reach the embryos [17]. In addition, using an *ex vivo* human placental perfusion model, it has been shown that polystyrene particles with diameter up to 240 nm are able to cross the placental barrier [18].

The results obtained in the present study provide evidence that 100 nm AuNPs, administered intraperitoneally, do not cause genotoxic damage in the bone marrow of adult mice but are genotoxic to both liver and peripheral blood of transplacentally exposed mice. In addition, transplacental exposure to AuNP-100 nm dys-regulated miRNA expression in the fetus lung and liver.

2. Materials and methods

2.1. Gold nanoparticles

AuNPs, with mean diameters of 40 nm and 100 nm, were supplied by BB International (Cardiff, UK) as a 0.01% colloidal suspension in H_2O. According to the producer, the standard deviation of nanoparticle diameter is less than 8%. The majority of the particles have spherical-like shape, but some polyhedral shapes can also be seen (not shown). The capacity of these nanoparticles to penetrate mammalian cells was evaluated by incubating for 24 h at 37 °C a suspension of HeLa cells (10^6 cells/ml medium) in the presence of AuNP-40 nm and AuNP-100 nm, at the concentration of 100 μl/ml. Transmission electron microscopy images showed that the AuNPs of either size are visible in the cell cytoplasm and are localized in endosomes near the nucleus (Fig. 1).

2.2. Mice

Female Swiss albino mice (H strain), obtained from the Animal Laboratory of the National Center of Oncology (Sofia, Bulgaria), weighing 28–30 g and aged 2.5–3 months, were mated with males of the same cross. Mating occurred overnight in a ratio of 1 male per 2 or 3 females, and on the following morning females were separated. This day was considered as a day 0 of gestation for those mice that had become pregnant. The pregnant mice were divided into 3 groups as follows: (1) untreated controls (2 dams); (2) mice treated with AuNP-40 nm (3 dams), and (3) pregnant mice treated with AuNP-100 nm (2 dams). The dams generated a total of 83 fetuses.

In parallel, 30 mice from the same strain (15 males and 15 females), weighing 28–30 g and aged 2.5–3 months, were used to study the possible clastogenicity of AuNPs in adults. These mice were divided into groups as follows: (1) untreated controls (5 males and 5 females); (2) mice treated with AuNP-40 nm (5 males and 5 females), and (3) mice treated with AuNP-100 nm (5 males and 5 females).

The mice were housed in plastic cages with wire tops and softwood bedding under standard laboratory conditions and free access to standard rodent chow and drinking water. Housing, breeding and treatment of mice were in accordance with national and institutional guidelines.

2.3. Treatment of mice

Pregnant mice were treated on days 10, 12, 14 and 17 of gestation with 1 ml/mouse of AuNP suspensions (either 40 nm or 100 nm), injected intraperitoneally (i.p), delivering an average dose of 3.3 mg/kg body weight. The corresponding control pregnant mice were injected with 1 ml/mouse distilled water. The frequency of

micronucleated polychromatic erythrocytes (MN PCEs) was evaluated in the liver of fetuses and in their peripheral blood on day 18 of gestation, as described earlier [19]. The number of liver fetuses analyzed for MN PCE frequency was as follows: 22 untreated fetuses, 33 fetuses treated transplacentally with AuNP-40 nm, and 28 fetuses treated transplacentally with AuNP-100 nm. In parallel, the PCEs/normochromatic erythrocytes (NCEs) ratio was calculated as an index for possible cytotoxicity. The frequency of MN PCEs was also analyzed in the bone marrow of the pregnant mice and of 30 additional adult mice (15 males and 15 females).

2.4. Histopathological analyses

Samples of fetal liver, kidney, lungs, brain and heart as well as samples of the organs of pregnant mice (heart, lungs, kidney, liver) and the placentas were isolated, fixed in 10% buffered formalin, cut into standardized sections, stained with hematoxylin and eosin, and subjected to standard histopathological examination.

2.5. Bone marrow processing

The pregnant mice and the other adult mice were sacrificed by cervical dislocation 24 h after the last treatment with AuNPs. Bone marrow smears (2 smears per mouse) were prepared by employing fetal calf serum, air-dried and stained with May–Grünwald–Giemsa [20]. From each pregnant or adult mouse, 4000 PCEs were scored for MN frequency.

2.6. Fetal liver processing

Single-cell suspensions of fetal livers from 83 mice were prepared in fetal calf serum by pipetting, and 2 smears per fetus were prepared, air-dried and stained with May–Grünwald–Giemsa [19–21]. At least 4000 PCEs per fetus were analyzed for MN frequency.

2.7. Fetal blood processing

Blood smears were prepared directly from a subset of 40 dissected fetuses (2 smears per fetus), air-dried at room temperature and stained with May–Grünwald–Giemsa. From each mouse, 4000 PCEs were screened for MN frequency. Only immature PCEs with homogenously blue-stained cytoplasm and without aggregated RNA were scored in fetal liver and fetal blood.

2.8. MiRNA expression analysis by microarray

MiRNAs were evaluated in triplicate in the lungs and livers of fetuses on day 18 of pregnancy, pooled within each one of the 3 experimental groups. RNA was extracted using the TRIzol Plus RNA Purification kit (Invitrogen, Carlsbad, CA). RNA integrity was evaluated by capillary electrophoresis (2100 Bioanalyzer, Agilent Technologies, Santa Clara, CA). miRNA samples were labeled using a commercially available kit (Label IT® miRNA Labeling Kit, Cy™3/Cy™5, Mirus Bio LLC, Madison, WI). The labeling reaction was performed at 37 °C for 1 h by adding 10× Labeling Buffer M, MB-grade Water and Label IT Cy™3 or Cy™5 Reagent to total RNA samples (1 μg). The reaction was stopped by adding 10 μl of 10× STOP Reagent. Labeled miRNAs were purified using the kit purification column, washed with buffer, eluted with the supplied elution buffer, and resuspended in hybridization solution.

The analysis of miRNA microarray expression was performed by using the miRCURY LNA microRNA Array, 7th generation (Exiqon, Woburn, MA, USA), which contains 3100 capture probes covering human, mouse and rat miRNAs. In particular, this array covers 1281 mouse miRNAs, which represents the 88.6% of the mouse miRNAs listed in miRBase 19. Microarray hybridization was performed in a hybridization station (HS4000-PRO, Tecan, Mannendorf, Switzerland) at 37 °C for 16 h. The hybridized microarrays slides were washed, dried by centrifugation and scanned at 535 and 635 nm by using a gas laser scanner (Scannerlite, Packard Bioscience, Billerica, MA, USA).

Table 1
Frequencies of MN PCE in liver and blood, and PCE/NCE ratio in the liver from mouse fetuses, as related to transplacental exposure to AuNPs.

Treatment	Liver		Blood
	MN PCE (‰)	PCE/NCE ratio	MN PCE (‰)
Untreated	3.6 ± 0.56	1.0 ± 0.03	4.8 ± 0.43
AuNP–40 nm	4.4 ± 0.30	1.1 ± 0.07	5.9 ± 1.06
AuNP–100 nm	8.0 ± 0.77[a]	1.5 ± 0.08	7.2 ± 0.22[a]

The results are means ± SE within the mice composing each experimental group.
[a] $P < 0.001$

2.9. Statistical analyses

Comparison between the experimental groups regarding cytogeneticity data was performed by means of the Student's *t*-test.

For microarray data, the data analysis was performed by GeneSpring® software version 7.2 (Agilent Technologies, Santa Clara, CA, USA). The spot background was subtracted from the spot intensity, and the resulting data were log-transformed and normalized both per gene and per array using the GeneSpring median-centered normalization option. Triplicate data were generated for each miRNA. The occurrence of ≥2-fold variations, accompanied by statistical significance ($P < 0.05$), as evaluated by ANOVA after Bonferroni's multiple testing correction, was assumed as a threshold for positivity. Global miRNA expression profiles were evaluated by scatter-plot analysis, volcano-plot analysis, and hierarchical cluster analysis. A GEO database number was requested.

3. Results

3.1. Pathology

Pathohistomorphological examination of the placentas and organs (heart, lung, kidney and liver) of the pregnant mice as well as the examination of fetal heart, lung, kidney, brain and liver did not reveal any significant morphological alteration as a result of the treatment of pregnant mice with AuNPs. An exception was the presence of a slight hyperplasia of the alveolar epithelium in the lungs of the fetuses transplacentally exposed to AuNP-100 nm. The mean body weight of the AuNP-100 nm-treated fetuses (129.4 ± 4.67 mg, mean ± SE) was significantly lower ($P < 0.05$) compared to the mean body weights of either control fetuses (147.7 ± 3.89 mg) or the fetuses exposed to AuNP-40 nm (152.5 ± 5.62 mg). The mean number of fetuses was not affected by treatment of the pregnant mice with AuNPs, being on an average 11 in both untreated mice and AuNP-40 nm-treated mice, and 14 in AuNP-100 nm-treated mice.

3.2. Cytogenetic damage

The data obtained indicated that the transplacental treatment of the mouse fetuses with AuNP-100 nm induced a significant enhancement of the frequency of MN PCEs in both fetal livers and peripheral blood, whereas AuNP-40 nm did not affect the frequency of MN PCEs (Table 1). No signs of toxicity to the erythroblasts were observed when evaluating the PCE/NCE ratio in fetal liver. No clastogenic effect was detected in the bone marrow either of pregnant mice or of male and female adult mice treated i.p. with AuNP-40 nm and AuNP-100 nm (data not shown). Likewise, there

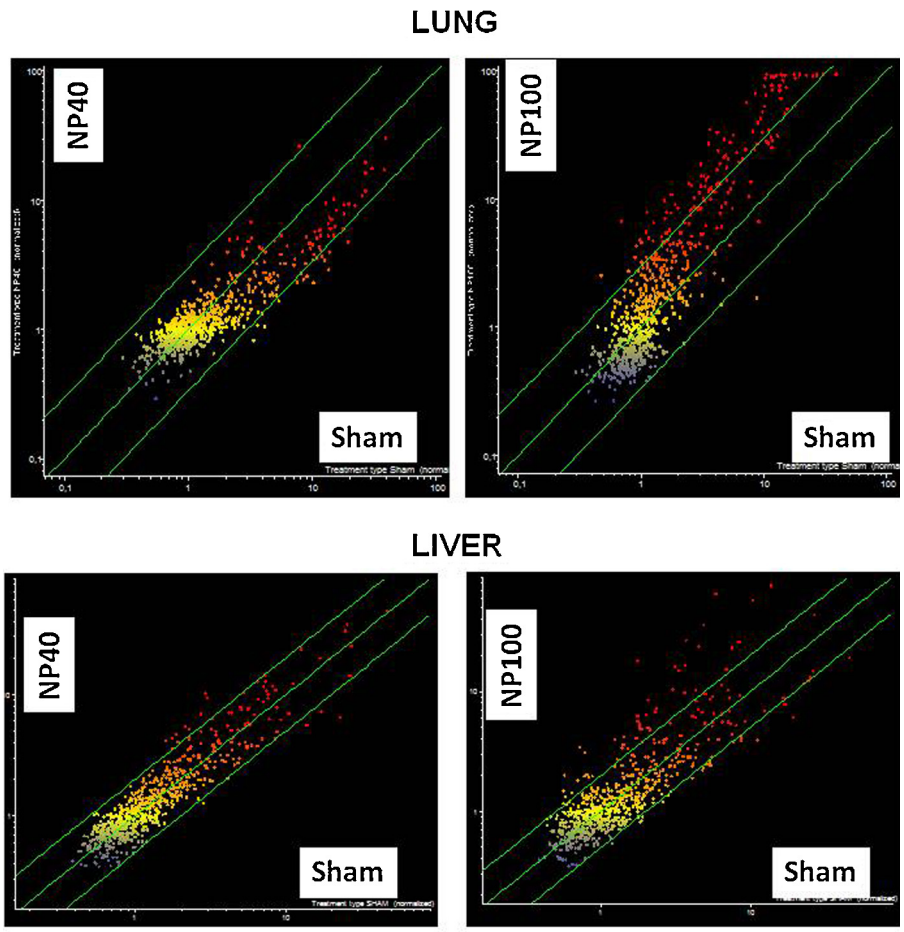

Fig. 2. Scatter-plot analyses showing the expression profiles of 1281 miRNAs in the fetal lung (upper panels) and liver (lower panels) of mice, either sham-treated (*X* axes) or transplacentally exposed to AuNP-40 nm or AuNP-100 nm (*Y* axes). Each miRNA is reported as a single dot located in the graph according to its expression level in the two compared experimental groups. MiRNAs having similar expression levels in the two groups fall inside the belt delimited by the diagonal green lines. MiRNAs with increased expression levels in the AuNP-40 nm- or AuNP-100 nm-treated mice are located above the diagonal green lines. MiRNAs with decreased expression levels in the AuNP-40 nm or AuNP-100 nm-treated mice are located below the diagonal green lines. The expression intensity of each miRNA is reported on a color scale (blue, low expression; yellow, intermediate expression; red, high expression). (For interpretation of the references to color in text, the reader is referred to the web version of this article.)

were no signs of cytotoxicity in the bone marrow of adult mice treated with AuNPs, as inferred from the PCE/NCE ratio (data not shown).

3.3. MiRNA expression profiles

3.3.1. Lung

Scatter-plot analyses of the microarray data indicated that AuNP-40 did not appreciably affect the miRNA expression profile in the lung (Fig. 2, upper left panel). Conversely, AuNP-100 nm modified the basal miRNA expression profile compared to the controls. This effect was mainly produced in terms of increasing the number of up-regulated miRNAs (Fig. 2, upper right panel). Hierarchical cluster analyses confirmed that the miRNA expression profile in the fetal lung of the AuNP-40 nm-treated mice was similar to that observed in sham-treated mice. In fact, their profiles are linked in the hierarchical dendrogram (Fig. 3, upper panel, columns 1 and 2 from left). Conversely, the miRNAs expression profile in the fetal lung of the AuNP-100 nm-treated mice was different from that observed in either sham-treated or AuNP-40 nm-treated mice. In fact, its profile departed from the other two profiles in the hierarchical dendrogram (Fig. 3, upper panel, column 3 from left).

Volcano plot analyses (not shown) indicated that, in the fetal lung, 1 miRNA was up-regulated and 13 miRNAs were down-regulated more than 2-fold in AuNP-40 nm-treated mice. However, none of these expression changes were statistically significant. Conversely, in the AuNP-100 nm-treated mice, 94 miRNAs were up-regulated and 1 miRNA was down-regulated more than 2-fold. Among these miRNAs, 28 (2.2%) varied their expression levels above the statistical significance threshold. The miRNAs identities and main regulated functions, as inferred from the TargetScan database (http://www.targetscan.org/), are reported in Table 2.

3.3.2. Liver

Scatter-plot analyses of the microarray data indicated that treatment of pregnant mice with AuNP-40 nm did not appreciably affect the miRNA expression profile in the fetus liver (Fig. 2, lower left panel). Conversely, AuNP-100 nm clearly modified the basal miRNA expression profile compared to the controls. The modification was mainly in terms of increasing the number of up-regulated miRNAs (Fig. 1, lower right panel).

Hierarchical cluster analyses confirmed that the miRNA expression profile in the fetal liver of the AuNP-40 nm-treated mice was similar to that observed in sham-treated mice. In fact, these profiles are linked in the hierarchical dendrogram (Fig. 3, lower panel, columns 1 and 2 from left). Conversely, the miRNA expression profile in the fetal liver of the AuNP-100 nm-treated mice was different from that observed both in sham-treated and AuNP-40 nm-treated mice. In fact, its profile departs from the other two profiles in the hierarchical dendrogram (Fig. 3, lower panel, column 3 from left).

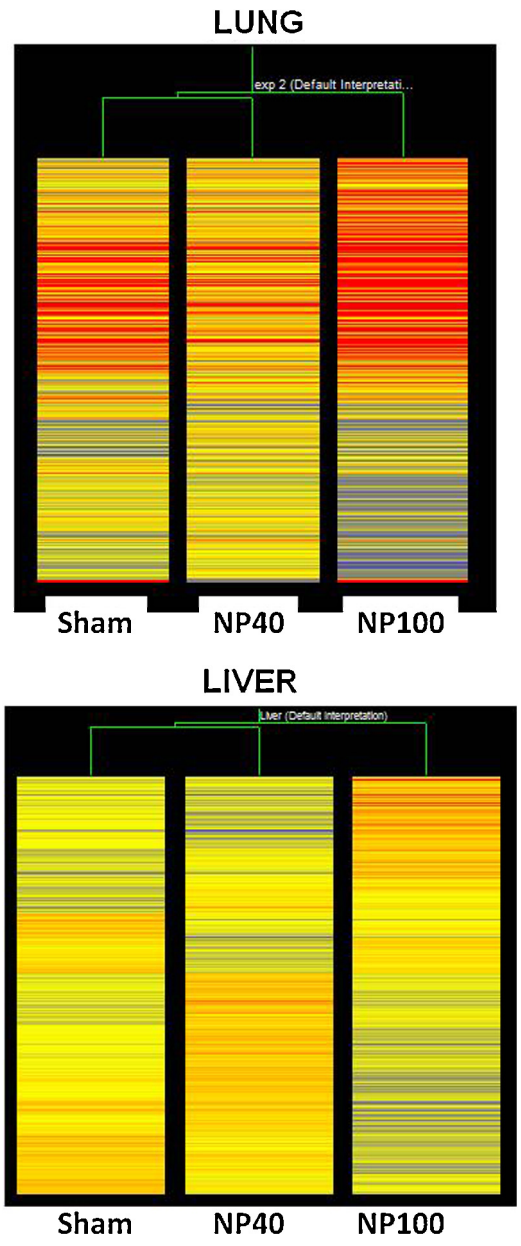

Fig. 3. Hierarchical cluster analysis reporting the expression profiles of 1281 miRNAs in the fetal lung (upper panel) or liver (lower panel) of mice, either sham-treated or transplacentally exposed to AuNP-40 nm or AuNP-100 nm. Each experimental group corresponds to a single column. Each horizontal line in the column is the expression level of a single miRNA, reported on a color scale. The green tree in the upper portion of the figure links those experimental groups having similar global miRNAs expression profiles. Both in the lung and the liver, this link occurs between the sham and the AuNP-40 nm profiles. The AuNP-100 nm profile is located away in the hierarchical tree. (For interpretation of the references to color in text, the reader is referred to the web version of this article.)

Volcano-plot analyses indicated that 8 miRNAs were up-regulated and 3 were down-regulated more than 2-fold in the liver of AuNP-40 nm-treated mice, but none of them was changed to a statistically significant extent. Conversely, in the AuNP-100 nm-treated mice, 47 miRNAs were up-regulated and 22 were down-regulated more than 2-fold. Among these miRNA, 5 (0.4%) varied their expression levels above the statistical significance threshold. Their identity and main regulated functions, as inferred from the TargetScan database (http://www.targetscan.org/), are reported in Table 2.

Table 2
Identities and functions of miRNAs whose expression levels were significantly ($P < 0.05$) altered by AuNP-100 nm in fetal mice lung and liver.

MiRNA identity	AuNP/Sham ratio	Regulated functions
Lung		
let-7a	7.1	Cell proliferation, oncogene (*RAS*) activation, angiogenesis
let-7f	3.9	Cell proliferation
let-7 g	4.8	Cell proliferation
miR-16	4.4	Apoptosis
miR-17	4.9	*PTEN*, DICER, TGF-beta, c-*MYC*
miR-26a	3.6	TGF-beta expression
miR-27a	2.1	Cell proliferation, stress response, protein repair
miR-98	3.7	NA
miR-126	2.7	Gene transcription
miR-130	2.9	Gene transcription, apoptosis
miR-143	4.4	NA
miR-183	4.3	Apoptosis, cell adhesion
miR-185	8.2	NA
miR-196a	3.6	TGF-beta
miR-297	4.8	Protein repair, cell cycle
miR-335	4.4	Insulin growth factor, cell proliferation, apoptosis
miR-423	2.1	NA
miR-466	7.0	Apoptosis, protein repair, cell proliferation
miR-467	7.3	Cell proliferation, Stress response
miR-494	4.0	NA
miR-615	0.3	NA
miR-665	2.5	NA
miR-669	6.0	NA
miR-690	4.2	Cell proliferation, cell adhesion
miR-691	4.8	NA
miR-709	4.1	Stress response, inflammation, lysosome activation
miR-877	7.7	NA
miR-883a	3.9	Tumor suppressing activity through phosphatidylinositol catabolism, protein synthesis, intracellular vesicle trafficking, protein repair, cell proliferation
Liver		
let-7a	2.22	Cell proliferation, k-*RAS* activation, apoptosis
miR-186	2.09	Apoptosis
miR-183	2.35	Apoptosis, cell adhesion
miR-328	2.54	NA
miR-1198	2.33	NA

NA, no target genes having a context score > 0.30 available in the TargetScan database.

Let-7a and miR-183 were the only miRNAs that were significantly up-regulated in both t lungs and livers of AuNP-100 nm-treated fetuses.

4. Discussion

The present study demonstrated for the first time that treatment of pregnant mice with AuNPs results in both clastogenic and epigenetic effects in fetal tissues. These results deserve attention, also because the dose used in our experiments was quite low, being approximately 1000 times lower than the LD_{50} of AuNPs in mice [22].

Under our experimental conditions, the treatment of pregnant mice with AuNPs did not produce any significant histomorphological change in the dam heart, lung, kidney or liver. In addition, no changes were apparent in the placenta or in the fetal heart, kidney, brain, or liver. Furthermore, no clastogenic activity was detectable in the bone marrow of adult mice of both genders treated with AuNPs of either 40 or 100 nm.

In previous studies in mice, no significant harmful effect was observed in organs of mice receiving i.p. injections of AuNPs of either 50 or 100 nm, whereas smaller particles, ranging between 8 and 37 nm, induced severe sickness and histopathological alterations in liver, lung, and spleen [23]. In another study, small AuNPs (15 nm) enhanced the frequency of MN PCEs in mouse bone marrow when administers orally at a dose of 320 mg/kg body weight, whereas doses of 80 and 160 mg were devoid of effects [24]. Thus, on the whole, it appears that the harmful effects of AuNPs in adult mice are size- and dose-dependent. Interestingly, it was also demonstrated that AuNPs can induce mutagenic effects in *Drosophila*, and the phenotypic modifications induced by these NPs could be transmitted to subsequent generations [25]. *In vitro* studies confirmed the potential harmful effects of AuNPs, which induced chromosomal aberrations [26], oxidative stress [27], mitochondrial damage [28], cytokinesis arrest and apoptosis [29] in cultured cells.

Little information is available regarding the interactions of NPs with biological barriers and in particular regarding their ability to interact with the placental barrier [30], although it has been demonstrated that both polystyrene particles [18] and AuNPs [17] can cross the placenta. It has also been shown that silica nanoparticles (70 nm) and TiO_2 nanoparticles (35 nm) can cause pregnancy complications when injected intravenously to pregnant mice [31]. Our results provide clear evidence that the i.p. treatment of pregnant mice with AuNP-100 nm, but not with AuNP-40 nm, produce both clastogenic effects and alterations of miRNA expression profiles in fetus tissues. Positivity of AuNPs in the MN test applied to fetus liver and peripheral blood PCEs contrasts with negativity of the same test in bone marrow PCEs of adult mice, among which the dams of the examined fetuses. This finding confirms that the transplacental MN test in fetal mouse liver is more sensitive than the standard MN test in adult mouse bone marrow [21] and highlights the fact that fetal hematopoietic cells are more susceptible than adult hematopoietic cells to the DNA damage induced by AuNPs.

The analysis of the majority of the mouse miRNAs identified thus far provided evidence that administration of AuNP-100 nm to pregnant mice alters miRNA expression profiles in fetus organs, whereas AuNP-40 nm failed to produce adverse effects in this experimental system. In particular, 5 miRNAs (0.4%) were significantly up-regulated in fetus liver. Thus, the transplacental exposure to AuNP-100 nm of liver cells, which in mouse fetus also bear hematopoietic functions, resulted both in clastogenic damage and in the up-regulation of miRNAs involved in cell proliferation, k-*RAS* activation, and apoptosis. Even more evident were the alterations of miRNA expression induced by AuNP 100 nm in fetus lung, which at the same time exhibited a mild hyperplasia of the alveolar epithelium. Of the 28 dys-regulated miRNAs in lung (2.2%), the only down-regulated miRNA was miR-615, whose target genes are unclear. In contrast, all remaining miRNAs were up-regulated following transplacental exposure to AuNP-100 nm. The most frequent targets for miRNA up-regulation were cell proliferation and adhesion, stress response, protein repair, apoptosis, and modulation of oncogenes (*RAS*, *MYC*), tumor suppressors (*PTEN*), and growth factors (TGF-beta, insulin growth factor).

Interestingly, miR-183 and let-7a were up-regulated in both lung and liver. The let-7 family is of special interest, since its expression has been found to be altered in neoplastic tissues and after treatment with some chemical carcinogens [32–36]. The potential ability of AuNPs to affect gene expression had previously been demonstrated in fetal lung fibroblasts [37] and in the liver of adult mice treated intravenously with 4 and 100 nm-sized PEG-coated AuNPs [38].

The size-dependence of the transplacental clastogenic and epigenetic effects observed in our study is of difficult interpretation. At least *in vitro*, our electron microscope findings showed that AuNPs of both 40 and 100 nm are uptaken by cells. According to some studies, the biodistribution and cytotoxicity of AuNPs are greater for particles of smaller size [12,16,39,40]. However, the size-dependence of AuNP toxicity in mice is complex, and it cannot be concluded that the smaller particles have greater toxicity. For instance, it was found that PEG-coated AuNPs of 10 and 60 nm are more toxic than those of 5 and 30 nm [41].

In conclusion, the present study demonstrated that the fetus is particularly vulnerable to the DNA damaging capacity of AuNPs and to the associated epigenetic alterations. This finding should be taken into due account in view of medical applications and other uses in humans of these nanomaterials.

Conflicts of interest

The authors declare that there are no conflicts of interest.

Acknowledgements

This study was supported by the Italian Association for Cancer Research (AIRC, grant no. 8909) and by the Bulgarian Ministry of Education, Youth and Science (SRF, grant DO-02-293).

References

[1] S. Lanone, J. Boczkowski, Biomedical applications and potential health risks of nanomaterials: molecular mechanisms, Curr. Mol. Med. 6 (2006) 651–663.
[2] S. Jain, D. Hirst, J. O'Sullivan, Gold nanoparticles as novel agents for cancer therapy, Br. J. Radiol. 85 (2012) 101–113.
[3] C. Medina, M.J. Santos-Martinez, A. Radomski, O.I. Corrigan, M.W. Radomski, Nanoparticles: pharmacological and toxicological significance, Br. J. Pharmacol. 150 (2007) 552–558.
[4] X.J. Liang, C. Chen, Y. Zhao, L. Jia, P.C. Wang, Biopharmaceutics and therapeutic potential of engineered nanomaterials, Curr. Drug Metab. 9 (2008) 697–709.
[5] N. Singh, B. Manshian, G.J. Jenkins, S.M. Griffiths, P.M. Williams, T.G. Maffeis, C.J. Wright, S.H. Doak, Nanogenotoxicology: the DNA damaging potential of engineered nanomaterials, Biomaterials 30 (2009) 3891–3914.
[6] R. Landsiedel, M.D. Kapp, M. Schulz, K. Wiench, F. Oesch, Genotoxicity investigations on nanomaterials: methods, preparation and characterization of test material, potential artifacts and limitations—many questions, some answers, Mutat. Res. 681 (2009) 241–258.
[7] E. Boisselier, D. Astruc, Gold nanoparticles in nanomedicine: preparations, imaging, diagnostics, therapies and toxicity, Chem. Soc. Rev. 38 (2009) 1759–1782.
[8] Y.H. Chen, C.Y. Tsai, P.Y. Huang, M.Y. Chang, P.C. Cheng, C.H. Chou, D.H. Chen, C.R. Wang, A.L. Shiau, C.L. Wu, Methotrexate conjugated to gold nanoparticles inhibits tumor growth in a syngeneic lung tumor model, Mol. Pharm. 4 (2007) 713–722.
[9] X. Huang, P.K. Jain, I.H. El-Sayed, M.A. El-Sayed, Gold nanoparticles: interesting optical properties and recent applications in cancer diagnostics and therapy, Nanomedicine 2 (2007) 681–693.
[10] J.C. Kah, K.W. Kho, C.G. Lee, C. James, R. Sheppard, Z.X. Shen, K.C. Soo, M.C. Olivo, Early diagnosis of oral cancer based on the surface plasmon resonance of gold nanoparticles, Int. J. Nanomed. 2 (2007) 785–798.
[11] P. Podsiadlo, V.A. Sinani, J.H. Bahng, N.W. Kam, J. Lee, N.A. Kotov, Gold nanoparticles enhance the anti-leukemia action of a 6-mercaptopurine chemotherapeutic agent, Langmuir 24 (2008) 568–574.
[12] K.L. Aillon, Y. Xie, N. El-Gendy, C.J. Berkland, M.L. Forrest, Effects of nanomaterial physicochemical properties on in vivo toxicity, Adv. Drug Deliv. Rev. 61 (2009) 457–466.
[13] H.J. Johnston, G. Hutchison, F.M. Christensen, S. Peters, S. Hankin, V. Stone, A review of the in vivo and in vitro toxicity of silver and gold particulates: particle attributes and biological mechanisms responsible for the observed toxicity, Crit. Rev. Toxicol. 40 (2010) 328–346.
[14] N. Khlebtsov, L. Dykman, Biodistribution and toxicity of engineered gold nanoparticles: a review of in vitro and in vivo studies, Chem. Soc. Rev. 40 (2011) 1647–1671.
[15] M. Tsoli, H. Kuhn, W. Brandau, H. Esche, G. Schmid, Cellular uptake and toxicity of Au55 clusters, Small 1 (2005) 841–844.
[16] Y. Pan, S. Neuss, A. Leifert, M. Fischler, F. Wen, U. Simon, G. Schmid, W. Brandau, W. Jahnen-Dechent, Size-dependent cytotoxicity of gold nanoparticles, Small 3 (2007) 1941–1949.
[17] M. Semmler-Behnke, S. Fertsch, G. Schmid, A. Wenk, W.G. Kreyling, Uptake of 1.4 nm versus 18 nm gold nanoparticles in secondary target organs is size dependent in control and pregnant rats after intratracheal or intravenous application, EuroNanoForum (2007) 102.

[18] P. Wick, A. Malek, P. Manser, D. Meili, X. Maeder-Althaus, L. Diener, P.A. Diener, A. Zisch, H.F. Krug, U. von Mandach, Barrier capacity of human placenta for nanosized materials, Environ. Health Perspect. 118 (2010) 432–436.
[19] R.M. Balansky, P.M. Blagoeva, Tobacco smoke-induced clastogenicity in mouse fetuses and in newborn mice, Mutat. Res. 223 (1989) 1–6.
[20] W. Schmid, The micronucleus test, Mutat. Res. 31 (1975) 9–15.
[21] R.J. Cole, N.A. Taylor, J. Cole, C.F. Arlett, Transplacental effects of chemical mutagens detected by the micronucleus test, Nature 277 (1979) 317–318.
[22] J.F. Hainfeld, D.N. Slatkin, T.M. Focella, H.M. Smilowitz, Gold nanoparticles: a new X-ray contrast agent, Br. J. Radiol. 79 (2006) 248–253.
[23] Y.S. Chen, Y.C. Hung, I. Liau, G.S. Huang, Assessment of the in vivo toxicity of gold nanoparticles, Nanoscale Res. Lett. 4 (2009) 858–864.
[24] E. Girgis, W.K. Khalil, A.N. Emam, M.B. Mohamed, K.V. Rao, Nanotoxicity of gold and gold–cobalt nanoalloy, Chem. Res. Toxicol. 25 (2012) 1086–1098.
[25] G. Vecchio, A. Galeone, V. Brunetti, G. Maiorano, L. Rizzello, S. Sabella, R. Cingolani, P.P. Pompa, Mutagenic effects of gold nanoparticles induce aberrant phenotypes in *Drosophila melanogaster*, Nanomedicine 8 (2012) 1–7.
[26] J.J. Li, S.L. Lo, C.T. Ng, R.L. Gurung, D. Hartono, M.P. Hande, C.N. Ong, B.H. Bay, L.Y. Yung, Genomic instability of gold nanoparticle treated human lung fibroblast cells, Biomaterials 32 (2011) 5515–5523.
[27] J.J. Li, L. Zou, D. Hartono, C.N. Ong, B.H. Bay, L.Y. Lanry Yung, Gold nanoparticles induce oxidative damage in lung fibroblasts in vitro, Adv. Mater. 20 (2007) 138–142.
[28] Y. Pan, A. Leifert, D. Ruau, S. Neuss, J. Bornemann, G. Schmid, W. Brandau, U. Simon, W. Jahnen-Dechent, Gold nanoparticles of diameter 1.4 nm trigger necrosis by oxidative stress and mitochondrial damage, Small 5 (2009) 2067–2076.
[29] B. Kang, M.A. Mackey, M.A. El-Sayed, Nuclear targeting of gold nanoparticles in cancer cells induces DNA damage, causing cytokinesis arrest and apoptosis, J. Am. Chem. Soc. 132 (2010) 1517–1519.
[30] M. Saunders, Transplacental transport of nanomaterials, Wiley Interdiscip. Rev. Nanomed. Nanobiotechnol. 1 (2009) 671–684.
[31] K. Yamashita, Y. Yoshioka, K. Higashisaka, K. Mimura, Y. Morishita, M. Nozaki, T. Yoshida, T. Ogura, H. Nabeshi, K. Nagano, Y. Abe, H. Kamada, Y. Monobe, T. Imazawa, H. Aoshima, K. Shishido, Y. Kawai, T. Mayumi, S. Tsunoda, N. Itoh, T. Yoshikawa, I. Yanagihara, S. Saito, Y. Tsutsumi, Silica and titanium dioxide nanoparticles cause pregnancy complications in mice, Nat. Nanotechnol. 6 (2011) 321–328.
[32] A. Izzotti, G.A. Calin, P. Arrigo, V.E. Steele, C.M. Croce, S. De Flora, Downregulation of microRNA expression in the lungs of rats exposed to cigarette smoke, FASEB J. 23 (2009) 806–812.
[33] B. Boyerinas, S.M. Park, A. Hau, A.E. Murmann, M.E. Peter, The role of let-7 in cell differentiation and cancer, Endocr. Relat. Cancer 17 (2010) F19–F36.
[34] T. Chen, A. Mally, S. Ozden, J.K. Chipman, Low doses of the carcinogen furan alter cell cycle and apoptosis gene expression in rat liver independent of DNA methylation, Environ. Health Perspect. 118 (2010) 1597–1602.
[35] K. Yamakawa, T. Kuno, N. Hashimoto, M. Yokohira, S. Suzuki, Y. Nakano, K. Saoo, K. Imaida, Molecular analysis of carcinogen-induced rodent lung tumors: involvement of microRNA expression and Krαs or Egfr mutations, Mol. Med. Rep. 3 (2010) 141–147.
[36] M.A. Parasramka, W.M. Dashwood, R. Wang, A. Abdelli, G.S. Bailey, D.E. Williams, E. Ho, R.H. Dashwood, MicroRNA profiling of carcinogen-induced rat colon tumors and the influence of dietary spinach, Mol. Nutr. Food Res. 56 (2012) 1259–1269.
[37] C.T. Ng, S.T. Dheen, W.C. Yip, C.N. Ong, B.H. Bay, L.Y. Lanry Yung, The induction of epigenetic regulation of PROS1 gene in lung fibroblasts by gold nanoparticles and implications for potential lung injury, Biomaterials 32 (2011) 7609–7615.
[38] W.S. Cho, S. Kim, B.S. Han, W.C. Son, J. Jeong, Comparison of gene expression profiles in mice liver following intravenous injection of 4 and 100 nm-sized PEG-coated gold nanoparticles, Toxicol. Lett. 191 (2009) 96–102.
[39] G. Sonavane, K. Tomoda, K. Makino, Biodistribution of colloidal gold nanoparticles after intravenous administration: effect of particle size, Colloids Surf. B: Biointerfaces 66 (2008) 274–280.
[40] C. Lasagna-Reeves, D. Gonzalez-Romero, M.A. Barria, I. Olmedo, A. Clos, V.M. Sadagopa Ramanujam, A. Urayama, L. Vergara, M.J. Kogan, C. Soto, Bioaccumulation and toxicity of gold nanoparticles after repeated administration in mice, Biochem. Biophys. Res. Commun. 393 (2010) 649–655.
[41] X.D. Zhang, D. Wu, X. Shen, P.X. Liu, N. Yang, B. Zhao, H. Zhang, Y.M. Sun, L.A. Zhang, F.Y. Fan, Size-dependent in vivo toxicity of PEG-coated gold nanoparticles, Int. J. Nanomed. 6 (2011) 2071–2081.